Available online at www.sciencedirect.com

ScienceDirect

Procedia Engineering 207 (2017) 1815–1820

Procedia Engineering

www.elsevier.com/locate/procedia

International Conference on the Technology of Plasticity, ICTP 2017, 17-22 September 2017, Cambridge, United Kingdom

Numerical and experimental investigations of the anisotropic transformation strains during martensitic transformation in a low alloy Cr-Mo steel 42CrMo4

Bernd-Arno Behrens[a], Anas Bouguecha[a], Christian Bonk[a], Alexander Chugreev[a,*]

[a] *IFUM - Institute of Forming Technology and Machines, Leibniz Universitaet Hannover, An der Universitaet 2, Garbsen 30823, Germany*

Abstract

Hot forming as a coupled thermo-mechanical process comprises of numerous material phenomena with a corresponding impact on the material behavior during and after the forming process. Within the subsequent heat treatment, possible rapid cooling of the hot formed parts leads to the diffusionless decomposition of austenite into martensite. In this context, in addition to the elastic, plastic and linear thermal strain components, complex isotropic as well as anisotropic transformation strains can occur. Irreversible anisotropic transformation strains account for the plastic deformation at the phase boundary between the emerging and the parent phase and are related to the transformation induced plasticity (TRIP or TP) phenomena. Moreover, TRIP strains can be reduced or amplified by varying the current stress state. These phenomena significantly contribute to the final residual stress state and may be responsible for the cost-intensive component defects arising due to thermal shrinkage. This study aims at developing an FE-based material model in order to describe and quantitatively visualize stress dependence of the transformation induced anisotropic strains for a typical forging steel 42CrMo4. The developed material model as well as the aspects of its implementation in a commercial FE-system (Simufact.forming) is presented. Consequently, the discussed material model is tested by comparison of experimental and numerical results with respect to resulting dilatation under various stress states.

Peer-review under responsibility of the scientific committee of the International Conference on the Technology of Plasticity.

Keywords: finite element analysis; transformation induced plasticity; multiscale material modelling, 42CrMo4

* Corresponding author. Tel.: +49-(0)-511-762-3405; fax: +49-(0)-511-762-3007.
E-mail address: chugreev@ifum.uni-hannover.de

1877-7058
Peer-review under responsibility of the scientific committee of the International Conference on the Technology of Plasticity.
10.1016/j.proeng.2017.10.944

Nomenclature

$d\varepsilon_{ij}^{el}$	elastic strain component
$d\varepsilon_{ij}^{pl}$	plastic strain component
$d\varepsilon_{ij}^{th}$	isotropic thermal strain component (due to thermal expansion/contraction)
$d\varepsilon_{ij}^{tr}$	isotropic transformation-related strain component (due to lattice structure change)
$d\varepsilon_{ij}^{tp}$	anisotropic transformation-related strain component (due to transformation plasticity)
ζ_k	total amount of a phase k (A for austenite, M for martensite)
$\zeta_{k,\max}$	maximal possible amount of a phase k (equal to the sum of rest austenite and already formed amount of k)
T_{Ms}	martensite start temperature
a_{γ}	averaged lattice constant for the current time step
σ_k	yield strength of a phase k
S_{ij}	deviatoric stress tensor
$\bar{\sigma}$	equivalent stress von Mises

1. Introduction and theory

In the context of constantly increasing technical requirements and intensified competition in the metal forming industry, thermo-mechanical metal processing is still gaining importance as one of the most cost-effective ways to produce high performance components. Thermo-mechanical rolling, hot stamping, near-net-shape as well as conventional closed-die hot forging and even welding and heat treatment processes are becoming parts of strongly integrated process chains [1]. As a consequence, complex material phenomena arising during the individual process steps interact and emphasize each other, decisively affecting the final component properties and making the virtual process design rather complicated. Numerous interactions between the mechanical, thermal and metallurgical fields can occur [2] (Fig. 1a). Particularly, in the case of closed-die hot forging, an appropriate numerical solution can help to predict and avoid the undesired component distortions arising from thermal and transformation related strains, which influence the final part quality especially regarding the increasingly tight manufacturing tolerances (Fig. 1c).

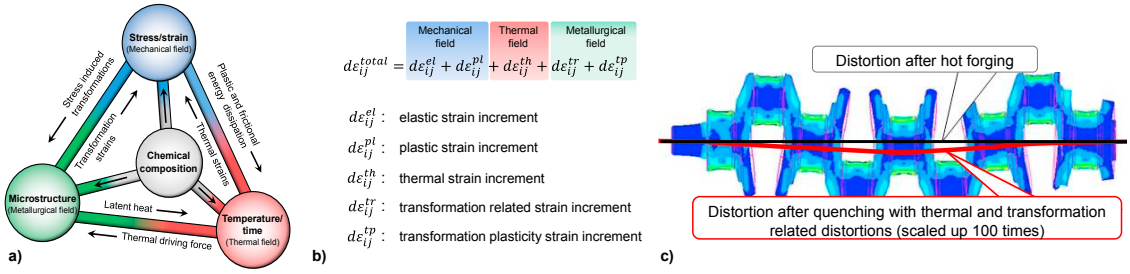

Fig. 1. (a) Interrelated thermo-mechanical-metallurgical material phenomena during thermo-mechanical processing of steel; (b) basic principles of the additive strain decomposition method and (c) distortion of an exemplarily forged part after heat treatment [3]

In order to ensure a realistic process simulation, an appropriate material modelling that provides a consistent description of polymorphic material behavior is essential. For this purpose, user defined FE-codes based on the additive strain decomposition (ASD) procedure [4] are commonly used for fully coupled thermo-mechanical-metallurgical FE-simulations, where the total strain increment is decomposed accordingly to Fig 1b.

2. Material model and implementation aspects

2.1. Implementation of user-defined thermo-mechanical-metallurgical material model in Simufact.forming

Based on the ASD method, a fully coupled thermo-mechanical-metallurgical material model with a focus on modelling the transformation induced plasticity effects in steel alloys was developed within this study and

implemented in a commercial FE code Simufact.forming with the help of user-subroutines according to the algorithm presented in Fig. 2a. The basic mathematical framework is based on the work of Simsir [5]. The algorithm was completely reworked avoiding the usage of common blocks in order to make it suitable for simulation of large strain problems requiring remeshing (e.g. closed-die hot forging) and was implemented into the Simufact.forming environment, which combines a user-friendly graphical interface with an open architecture of MSC.Marc-solver and thus is suitable for almost all scientific simulations in the field of metal processing.

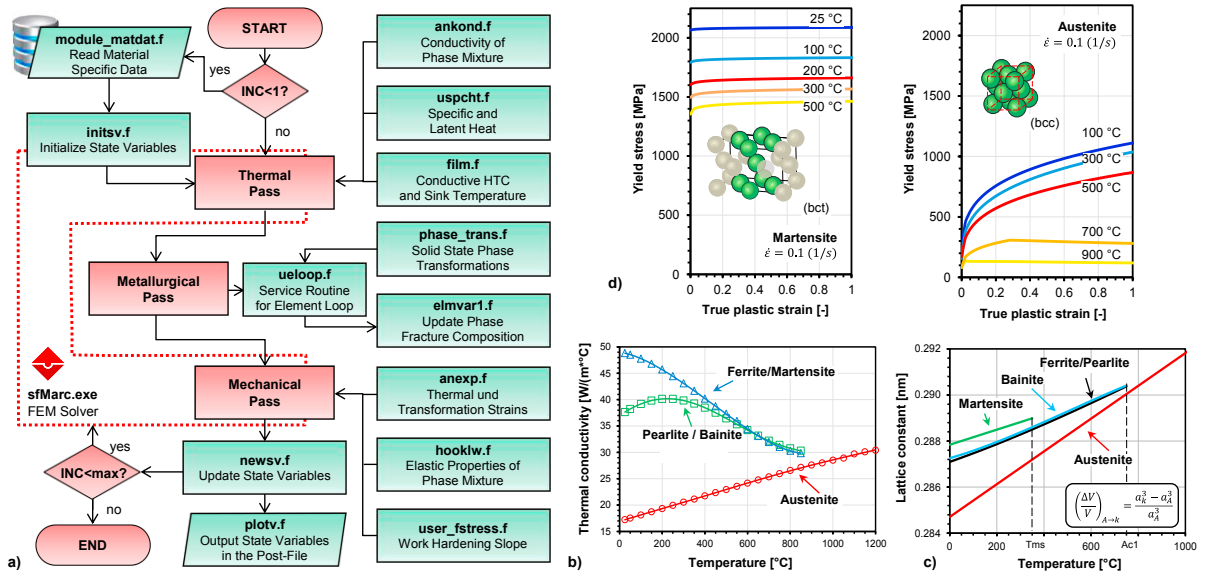

Fig. 2. (a) Schematics of the implementation algorithm; phase- and temperature-dependent (b) thermal conductivity; (c) lattice constants and (d) flow stress used for numerical study

2.2. Modelling the thermal field

In general, solution algorithm comprises three main steps (thermal, metallurgical and mechanical) according to the simulation fields in Fig. 1a. After the material specific data is read from the user-defined module (module_matdat.f), the simulation starts with an initialization of user-defined state variables (e.g. initial phase composition equal to 100% austenite). During the thermal step, user-subroutines ankond.f and uspcht.f are called in order to calculate instantaneous thermal properties of the current phase mixture accordingly to Eq. 1.

$$P(T,\zeta_k) = \sum_{k=1}^{5} P_k(T) \cdot \zeta_k \tag{1}$$

where $P(T,\zeta_k)$ is a thermal property of the phase mixture ζ_k at a current temperature T. Temperature as well as phase dependent material properties for 42CrMo4 can be found in literature [6], computed using thermodynamic software (e.g. JMatPro [7]) or determined experimentally. Phase-dependent thermal and mechanical material data used in this study for the high strength steel 42CrMo4 steel is based on JMatPro calculations [8] and is exemplarily presented in Fig. 2b, 2d. Phase and temperature dependent lattice constants used for the volume change calculations were determined based on the chemical composition using the model of Wildau and Hougardy [8], see Fig. 2c.

2.3. Modelling the metallurgical field during martensitic transformation

After the thermal calculation, a fictitious metallurgical step is integrated via a service subroutine ueloop.f, which is called in key element loops over the solution progress according to internal variables “ipass” and “iflag”.

Incremental phase transformations are calculated within the subroutine phase_trans.f and then saved in ueloop.f. For the prediction of phase transformation kinetics in the field of metal forming, a large variety of physical as well as semi-empirical mathematical models have been introduced [10]. Generally, the phase transformations can be classified into diffusion controlled (forming ferrite, pearlite or bainite) and diffusionless (martensite) transformations [11]. The current study is focused on the modelling of martensitic transformation, thus Koistinen and Marburger equation, as expressed by Eq. 2, is incorporated for the calculation.

$$\zeta_M = \zeta_{M,\max} \cdot \left(1 - e^{\alpha \left(T_{Ms} - T\right)^{kM}}\right) \tag{2}$$

where α and kM are material specific coefficients defined as a function of T_{Ms} [12].

2.4. Modelling the mechanical field

Coupling thermal and metallurgical interactions to mechanical field is solved within the user_fstress.f, hooklw.f and anexp.f subroutines, where user-defined flow stress, elastic properties as well as anisotropic thermal and transformation strains are computed. Phase and temperature dependent flow stress model is incorporated in user_fstress.f and is based on the current phase mixture and the flow stress of each particular phase, which are then combined via a linear rule of mixture analog to Eq. 1. Isotropic thermal strains due to thermal shrinkage and phase transformations are computed within anexp.f based on the lattice constants (Fig. 2c) as discussed in [13]:

$$d\varepsilon_{ij}^{th+tr} = d\varepsilon_{ij}^{th} + d\varepsilon_{ij}^{tr} = \left(\frac{a_n^{new}}{a_n^{old}} - 1\right) \cdot \delta_{ij} \tag{3}$$

Anisotropic transformation strains were also incorporated in anexp.f and are calculated based on the commonly used model of Leblond [14] as expressed by Eq. 4.

$$d\varepsilon_{ij}^{tp} = C_{TP} \cdot \frac{1}{\sigma_A^Y} \cdot \left(\frac{\Delta V}{V}\right)_{A \to k} \cdot h\left(\frac{\bar{\sigma}}{\sigma_{total}^Y}\right) \cdot \psi'\left(\zeta_k\right) \cdot d\zeta_k \cdot S_{ij} \tag{4}$$

where C_{TP} and $\psi'\left(\zeta_k\right)$ represent TRIP coefficient and derivation of the TRIP saturation function, respectively (e.g. $C_{TP} = 3$ and $\psi'\left(\zeta_k\right) = -\ln\zeta_k$ [14]). After the incremental solution is achieved, the final output is executed via newsv.f and plotv.f routines. In order to save internal user-defined variables between the iterations, service subroutines (e.g. elmvar1) were used. Further detailed information on the particular application of MSC.Marc user-routines can be found in [16]. The presented material model was programmed in FORTRAN and integrated in Simufact.forming-solver accordingly to Fig. 2a. It should be mentioned that already existing implementation schemes are to the best knowledge of the authors either closed commercial codes without a possibility to adjust the individual computation models (e.g. Deform-HT) or are not suitable for large strain problems (e.g. due to the lack of remeshing [17]). By means of the presented implementation scheme it is possible to examine and customize all the individual parts of the FE-code and solve large strain problems as well (e.g. closed-die hot forging simulation).

3. Case study

A quenching-deformation dilatometer system DIL 805A/D+T (TA Instruments Inc.) was used for thermo-mechanical physical simulations (Fig. 4a). During the experimental tests, middle segment (D5 x L10 mm) of cylindrical specimens made of 42CrMo4 was undergoing the time-force-temperature profile as depicted in the Fig. 4b. After an austenitisation at 950 °C for 5 minutes, the material was cooled down along a nearly exponential time-temperature route with cooling rates in the range of -75…-8 °C/s. In order to simulate the TRIP effect, constant

tensile or compressive loads (±F) were applied at the moveable support mount at a temperature of 400 °C just before the martensitic transformation. Further details about the experimental procedure can be found in [18].

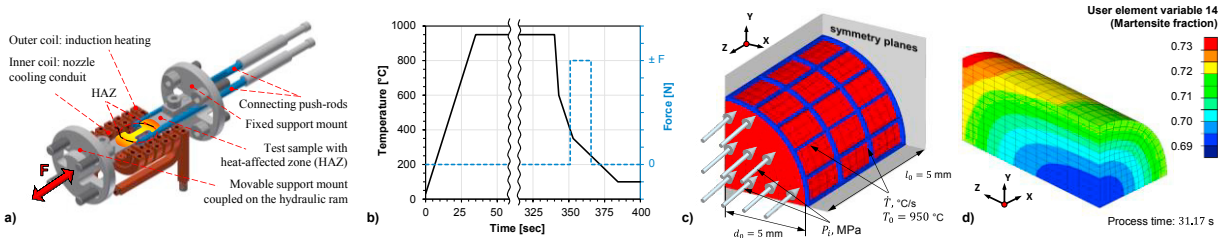

Fig. 4. (a) Experimental setup used for physical simulation; (b) time-temperature-force profile; (c) schematics of the used FE-model and (d) an exemplarily plot of the martensite fraction after 31 s of cooling

In order to verify whether the presented model and implementation scheme is suitable for description of the transformation plasticity phenomena in 42CrMo4, a one-eighth FE-model of the experimental tests was built up consisting of approx. 1500 hex-elements (Fig. 4c). Instead of axisymmetric model, a three-dimensional approach was used in order to simplify the portability of the developed FE-code to more complex problems. The applied forces as well as thermal boundary conditions were modelled based on the experimentally measured time-force-temperature profiles.

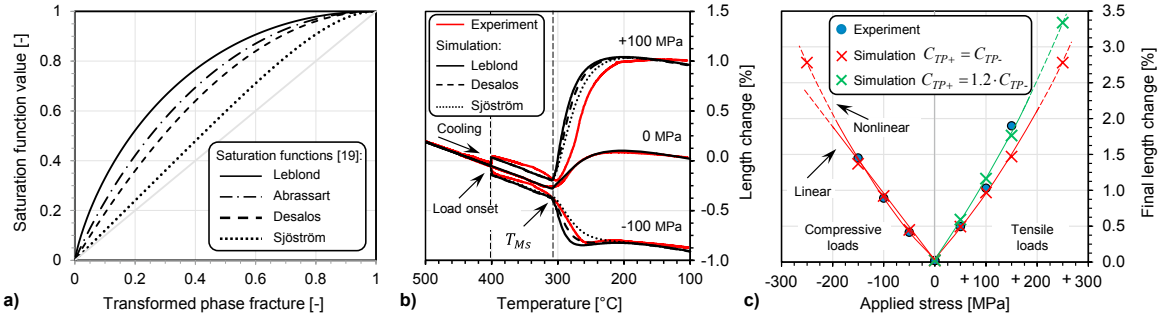

Fig. 5. (a) Common TRIP saturation functions; (b) comparison between experimental and numerical longitudinal dilatations; (c) comparison between measured and calculated final length changes

The resulted longitudinal dilatations from experimental (red) as well as numerical (black) tests are presented in Fig. 5b. After the linear contraction due to the cooling from 950 °C, an elastic length change due to the load onset at 400 °C can be observed in the experiment. Afterwards, the stress free specimens show distinct volume change due to martensitic transformation under 310 °C with a final dilatation after the entire heating-cooling cycle nearly equal to zero at 100°C. In contrast to these, load assisted tests both under compressive (-100 MPa) and tensile (+100 MPa) stresses demonstrate irreversible dimension changes of -0.89 % and 1.03 %, respectively. A more pronounced TRIP strain was observed also for other tensile loads with a nonlinear growth related to the increase of the applied tensile load (Fig. 5c). Thus, besides the total amount of deviatoric stress the TRIP model must also consider current stress state e.g. via stress state dependent TRIP coefficient. For example, an additional simulation sequence with a 20 % higher TRIP coefficient for tensile stress states C_{TP+} compared to compressive ones have been carried out and have shown a better approximation especially for the 150 MPa stress case (Fig. 5c). However, even if the final dimension changes are in a good agreement with the experimental data, the predicted progress of the TRIP strain during the transformation (see Fig. 5b, area between 250 and 300 °C) may be further enhanced e.g. by adjusting the employed TRIP saturation function in Eq. 5. In order to clarify the influence of different saturation functions, three common ones responsible for a fast (Leblond), slow (Sjöström) as well as moderate (Desalos) TRIP propagation (Fig. 5a) has been employed within the numerical study. Under the compressive load the model of Desalos has shown better approximation compared to the models of Leblond and Sjöström (Fig. 5b). On the contrary, in the tensile load case

all the models show a very similar behavior compared to the experimental dilatation curve but have a significant offset of approx. 20 °C. It may be explained by a stress dependency of the martensitic start temperature [5], which has been not considered yet, but after an extensive experimental study can be easily implemented in the model for a more precise prediction. The resulting dimensional changes show a nearly linear dependence on the applied load at least for low stresses as discussed in [14]. The implemented model predicts a nonlinear increase of the TRIP strain for higher stress states (e.g. ±250 MPa as shown in Fig. 5c). Thus, an additional study for high stress states would be also expedient but due to an overlapping between the macroscopic plastic flow of the hot austenite with the occurring TRIP strain, it requires further development of the experimental setup. In general, it can be stated that the proposed code delivers a sufficiently accurate approximation of the experimental data particularly regarding the final dimensional changes and can be easily extended according to the user's requirements (e.g. stress state dependency of the TRIP coefficient as shown in Fig. 5c).

4. Conclusions and summary

The presented implementation scheme combining a user-friendly interface of Simufact.forming with the open architecture of MSC.Marc-solver is rather universal and can be easily adapted to the user's needs (e.g. testing different saturation functions, etc.) or used for diverse thermo-mechanical process simulations (e.g. hot forging, hot stamping, coupled heat treatment, welding or tool analysis [18]). In this context, future investigations will aim at further improvement of the prediction accuracy of the developed FE-code involving backflow effects in TRIP as discussed in [5] and testing the model on a more complex industrial process (hot forging with an integrated heat treatment).

Acknowledgements

The authors wish to express sincere thanks to the German Research Foundation (DFG) for financial support of the research project BE1691/142-1 "Simulation of the undesired distortions in hot forged and subsequently heat treated components considering the impact of unsteady stress state on the transformation plasticity".

References

[1] B. Verlinden, J. Driver, I. Samajdar, R. D. Doherty, Thermo-mechanical processing of metallic materials, Vol. 11, Elsevier Science, 2007.
[2] B.-A. Behrens, W. Bleck, Fr.-W. Bach, E. Brinksmeier, U. Fritsching, M. Liewald, H.-W. Zoch, EcoForge: Resource-efficient process chains for high performance parts, Key Eng. Mat., 504-506 (2012) 151-156.
[3] Courtesy of DKK Co., Ltd., Japan: https://www.denkikogyo.co.jp/en/business/hf/technology/simulation2.html.
[4] S. Denis, E. Gautier, A. Simon, G. Beck, Stress-phase-transformation interactions, Mat. Science and Technology 1 (1985) 805-814.
[5] C. Simsir, 3D finite element simulation of steel quenching in order to determine the microstructure and residual stresses, PhD, 2008.
[6] G. Besserdich, Untersuchungen zur Eigenspannungs- und Verzugsausbildung beim Abschrecken von Zylindern aus den Stählen 42CrMo4 und Ck45 unter Berücksichtigung der Umwandlungsplastizität, PhD, 1993.
[7] N. Saunders, Z. Guo, A. Miodownik, J.-P. Schillé, Using JMatPro to model materials properties and behavior, J. Min. Met. Mat. Society 55 (2003) 60-65.
[8] Simufact.engineering GmbH, Material database for thermo-mechanical simulations, 2016.
[9] M. Wildau, H. Hougardy, Zur Auswirkung der Ms-Temperatur auf Spannungen und Maßänderungen, HTM 42 (1987) 261-268.
[10] C. H. Gur, J. Pan, Handbook of Thermal Process Modelling of Steels, CRC Press, 2009.
[11] J. Rohde, A. Jeppsson, Literature review of heat treatment simulations, Scandinavian Journal of Metallurgy 29 (2000) 47-62.
[12] H. Hougardy, K. Yamazaki, An improved calculation of the transformation of steels, Steel Research 57 (1986) 466–471.
[13] P. Olle, Numerisch und experimentalle Untersuchungen zum Presshaerten, PhD, 2010.
[14] J. Leblond, Mathematical modelling of transformation plasticity in steels, Int. J. Plast. 5 (1989) 573-591.
[15] F. Fischer, Q. Sun, K. Tanaka, Transformation-Induced Plasticity (TRIP), App. Mech. Rev. 49 (1996) 317-364.
[16] MSC Software Inc., MSC.Marc user documentation, Volume D: user subroutines and special routines, 2013.
[17] A. Schneidt, A. Mahnken, Modellierung der Umwandlungsplastizität und Viskoplastizitaet, Proc. in App. Math. and Mech. 8 (2008) 461-462.
[18] B.-A. Behrens, A. Bouguecha, C. Bonk, A. Chugreev, Experimental investigations on the transformation induced plasticity in a high tensile steel under varying thermo-mechanical loading, Computer Methods in Materials Science 17 (2017) 36-43.
[19] M. Dalgic, G. Löwisch, H.-W. Zoch, Beschreibung der Umwandlungsplastizität auf Grund innerer Spannungen während der Phasentransformation des Stahls 100Cr6, HTM 61 (2006) 222-228.
[20] B.-A. Behrens, A. Bouguecha, M. Vucetic, A. Chugreev, Advanced Wear Simulation for Bulk Metal Forming Processes, MATEC 80 (2016).